Investigation of the Reaction between Fe_2O_3 and Si Activated by Ball Milling

Giorgio Concas[a], Francesco Congiu[a], Anna Corrias[b], Carlo Muntoni[a], Giorgio Paschina[b], and Daniela Zedda[b]

[a] Dipartimento di Scienze Fisiche, Universitá di Cagliari and Istituto Nazionale di Fisica della Materia, Via Ospedale 72, I-09124 Cagliari, Italy.
[b] Dipartimento di Scienze Chimiche, Universitá di Cagliari, Via Ospedale 72, I-09124 Cagliari, Italy.

Z. Naturforsch. **51a**, 915–922 (1996); received April 1, 1996

The path of the reaction between Fe_2O_3 and Si, activated by high energy ball milling, has been investigated by X-ray diffraction and Mössbauer spectroscopy. Hematite reduction involves oxygen transfer from Fe to Si with the formation of intermediate phases containing Fe(II), which are then reduced to Fe(0). A steady state is reached in the milling process where the reduction of stoichiometric amounts of Fe_2O_3 and Si is not complete and an amount of Fe(II) in an amorphous matrix still remains. The same intermediate compounds are also observed in the milling process of mixtures with higher Fe_2O_3/Si molar ratio.

Key words: Mechanosynthesis, Nanocomposite, Reduction reaction, Mössbauer spectroscopy, X-ray diffraction.

Introduction

In the field of composite materials, nanocomposites consisting of metal particles embedded in either an insulating matrix or an immiscible metallic matrix have recently found much interest [1–6] because of their peculiar electric, magnetic and catalytic properties [1, 2, 7–10].

Several methods are suitable for the preparation of these materials [2, 4]; among them high energy ball milling seems to be a particularly versatile method [11–19]. This technique can be applied to the preparation of nanocomposites, either through an intimate mixing of the metal and matrix component [11–13] or through the activation of solid state reactions, in which the nanocomposite is the final product [14–19].

The most extensively experimented solid state reactions are those involving oxygen transfer from metal oxides to aluminium [15, 16, 18]. Also Mg, Zn, Fe, B, and Si have been used as oxygen acceptors [14, 15, 17–19].

The complete transfer of oxygen is not always possible; in this case a steady state is reached in which the desired products are accompanied by by-products. It is therefore of interest to study the reaction path in such systems in order to fully exploit the capabilities of this preparation method.

The aim of this work is to investigate the intermediate phases and final products of the reaction between Fe_2O_3 and Si by means of X-ray diffraction and Mössbauer spectroscopy.

Reprint requests to Prof. Giorgio Paschina,
Fax +39 70 66 92 72.

1. Experimental Procedure

Three mixtures of Si (Fluka 99.9%) and Fe_2O_3 (Carlo Erba 99%) powders were milled in a Fritsch Pulverisette 5 planetary ball mill. The weight of the reagents was adjusted according to the following Fe_2O_3/Si molar ratios:

$$2\,Fe_2O_3/3\,Si\,,\quad 4\,Fe_2O_3/3\,Si\,,\quad 12\,Fe_2O_3/3\,Si\,,$$

where the first molar ratio corresponds to the complete exchange reaction stoichiometry.

The metal volume fractions in the samples, calculated considering a complete reduction of Fe_2O_3 to Fe, are 26%, 41% and 68%, respectively; the samples will be hereafter referred to as 26 F, 41 F, and 68 F; the suffix xh, where x indicates the milling hours, will be used when required.

20 grams of each mixture were sealed in a 250 ml stainless steel vial with balls of the same material (diameter 8 mm) in argon atmosphere. Full/void volume

0932-0784 / 96 / 0800-0915 $ 06.00 © – Verlag der Zeitschrift für Naturforschung, D-72072 Tübingen

ratio and ball/powder weight ratio were fixed to 1/10 and 10/1, respectively; for the 26 F sample the rotation speed of the mill was initially set to 250 rpm and increased to 290 rpm after 5 h milling. For the other two samples the rotation speed was kept at 290 rpm during the whole milling process. Overheating was prevented by a cold air jet and by alternating milling and rest periods at 5 minute intervals.

At the end of the milling process an additional thermal treatment in H_2 flux at 450 °C was carried out on the 26 F, 41 F and 68 F samples for 1.5, 3 and 5 hours, respectively.

The effect of milling on the powder mixtures was monitored by means of X-ray diffraction (XRD) and Mössbauer spectroscopy on small portions of the powders, sampled at different milling times in argon atmosphere.

The XRD spectra were recorded in reflection mode on a $\theta-\theta$ Seifert diffractometer in the range $10° < \theta < 60°$ using CuK_α radiation ($\lambda = 1.5406$ Å).

The XRD line profile analysis was performed on (110) and (220) α-Fe reflections in the 26 F 48 h sample according to the Warren-Averbach method [20] in order to determine the average crystallite size and strain. Peaks were deconvoluted from instrumental effects using a standard Si sample.

The Mössbauer absorption spectra were obtained in the standard transmission geometry, using a source of ^{57}Co in rhodium (37 MBq). Calibration was performed using a 25 μm thick natural α-Fe foil; the isomer shifts are referred to α-Fe.

The measurements were carried out at room temperature on powder samples contained in a Plexiglas holder. The iron surface density of the absorber for the 26 F samples is 14 mg/cm^2, except for the 26 F 5 h sample (10 mg/cm^2). Measurements on the 41 F and 68 F samples were performed by mixing the samples with graphite (weight ratio 1:1); the resulting iron surface density is 12 mg/cm^2.

The absorption spectra of the 26 F and 41 F samples were analysed by fitting the data by Lorentzian line shapes. The same fitting procedure, applied to the spectra of 68 F samples, did not give satisfactory results owing to the nanocrystalline structure of the oxides, as discussed in the following.

A quadrupole doublet with the typical features of an amorphous material was present in all the examined spectra. The two absorption peaks have different amplitude and full width at half maximum (FWHM), but the same area; moreover the FWHM's are two times larger than that of a crystalline material. As first approximation, this doublet was fitted using two lines of Lorentzian shape and the same area, in order to take the asymmetry of the doublet into account.

The crystalline component was subtracted in the spectrum of 26 F 48 h sample, and the remaining amorphous component was fitted using the method proposed by Hesse and Rubartsch [21] and improved by Wivel and Mørup [22]. This method makes use of a set of Lorentzian quadrupole doublets with fixed width and splitting; it computes the contribution of each curve to the absorption spectrum by a least squares fitting procedure, allowing for the empirical linear relationship between isomer shift, δ, and quadrupole splitting, Δ, of each doublet [21, 22],

$$\delta = \xi + \eta * \Delta \,. \tag{1}$$

The program gives the best fit values of the free parameters ξ and η and the probability distribution of the quadrupole splitting. Following Wivel and Mørup [22], minimisation is performed using the Lagrangean multipliers γ and β's, which control the smoothing and the end point behaviour of the distribution profiles, respectively.

2. Results

Figure 1 shows the XRD spectra corresponding to the most meaningful steps of the milling process carried out on the 26 F sample.

The spectra after 1 and 5 h milling are similar. Both of them present peaks due to the starting crystalline phases Fe_2O_3 and Si [23]; the peaks are slightly broader in the spectrum after 5 h, which also indicates the presence of some magnetite Fe_3O_4 [23]. The most intense peak of Fe_3O_4 is centered at 17.7° and cannot be resolved from the hematite peak at 17.8°; nevertheless, the change in the intensity ratio between the peaks at 16.6° and 17.8° and the presence of the faint peaks at 15.0° and 21.5° suggests that Fe_3O_4 is produced at this milling stage.

After 5 h the milling speed was increased from 250 to 290 rpm because the process seemed to evolve too slowly. After 5 additional hours, in the 26 F 10 h spectrum peaks due to α-Fe [23] begin to appear, together with other peaks due to an intermediate phase identified as fayalite (Fe_2SiO_4) [23]. A faint peak, ascribable to wuestite (FeO) [23], is also detectable at $\theta = 21.0°$.

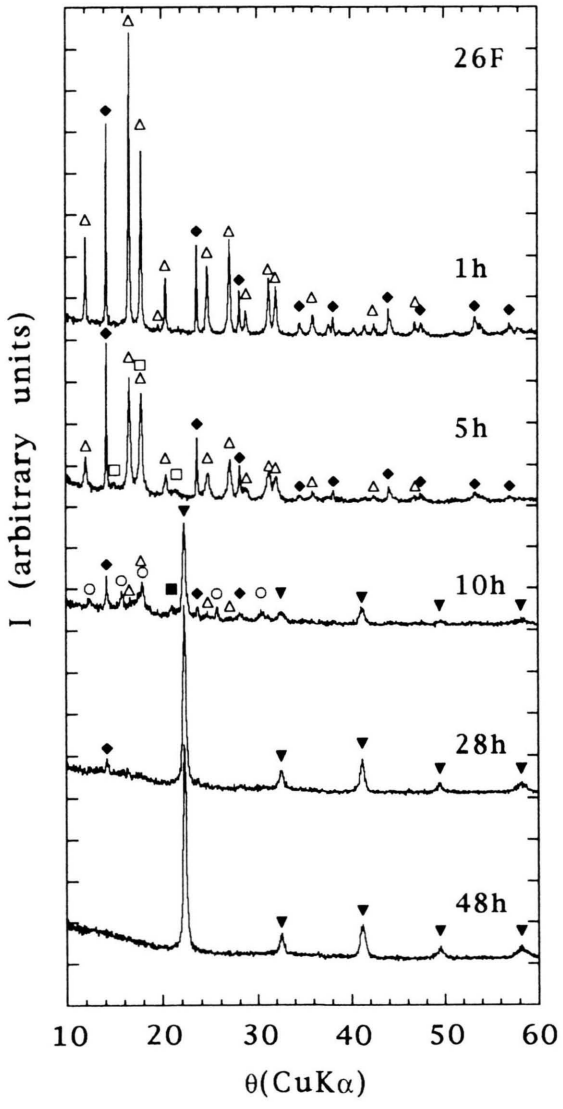

Fig. 1. X-ray diffraction spectra at selected milling times for the 26 F sample. (◆) Si, (△) Fe_2O_3, (□) Fe_3O_4, (■) FeO, (○) Fe_2SiO_4, (▼) Fe.

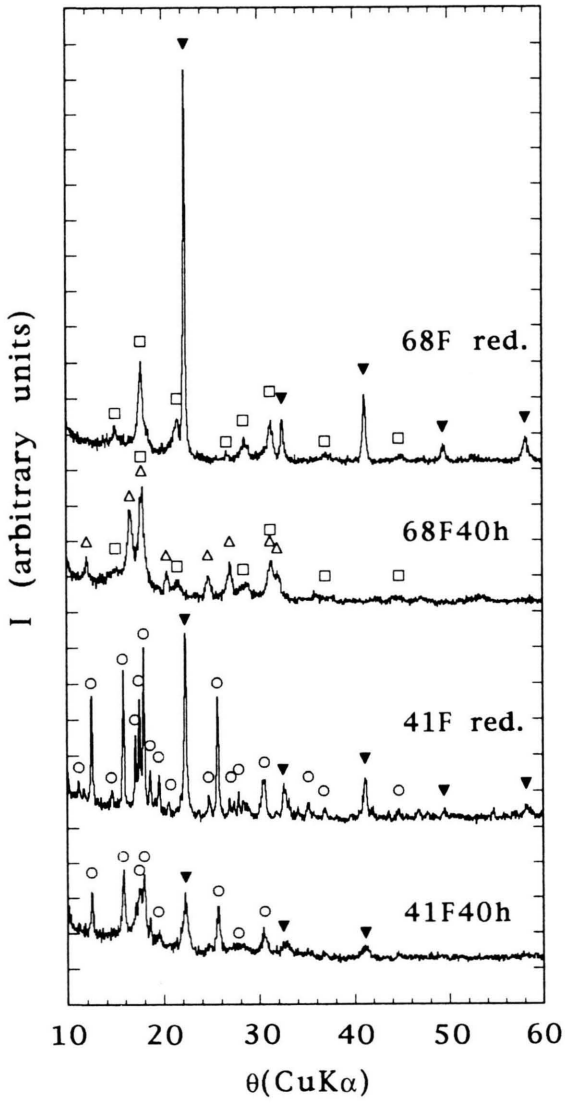

Fig. 2. X-ray diffraction spectra at selected milling times for the 41 F and 68 F samples at the end of the milling process and after an additional thermal treatment in H_2 flux. (△) Fe_2O_3, (□) Fe_3O_4, (○) Fe_2SiO_4, (▼) Fe.

Only traces of the peaks of the starting components are still present.

The peaks due to fayalite, wuestite, hematite and silicon disappear with further milling; only α-Fe peaks are detectable in the 26 F 48 h spectrum. At this stage the milling was interrupted because no significant variation in the XRD pattern was observed with respect to 26 F 43 h (not reported). No peaks due to any SiO_2 crystalline form appear in any of the milling steps.

The α-Fe average crystallite dimensions in the 26 F 48 h sample, obtained by the Warren Averbach method, are about 10 nm with 0.35% strain.

Figure 2 shows the diffraction spectra of the samples 41 F and 68 F prepared by milling the powders with higher Fe_2O_3/Si ratios. The spectra of the sam-

ples after an additional thermal treatment in H_2 flux are also reported. The 41 F 40 h spectrum does not show any peak of the starting powders, while peaks due to Fe_2SiO_4 are present together with α-Fe peaks. In the 68 F 40 h spectrum, peaks due to Fe_2O_3 are still clearly visible, accompanied by Fe_3O_4 peaks. The thermal treatment in H_2 flux does not induce the formation of new phases in the 41 F sample; the α-Fe and Fe_2SiO_4 peaks become slightly sharper due to an increase of their amount and crystallite dimensions. On the other hand, the thermal treatment of the 68 F 40 h sample induces larger effects. In fact, in the corresponding spectrum α-Fe peaks clearly appear, replacing the Fe_2O_3 one. The Fe_3O_4 peaks are only slightly modified by thermal treatment.

In Fig. 3 the Mössbauer absorption spectra of the 26 F samples, at the same milling times as the XRD spectra, are shown. In Table 1 the results of the least squares fits of the spectra (by using lines of Lorentzian shape) are reported. The values of isomer shift referred to α-Fe (δ), quadrupole splitting (Δ), internal magnetic field (B) and half width at half maximum ($\Gamma_1/2$ and $\Gamma_2/2$) are reported. The contribution of each component to the total absorption area is also shown. Owing to overlap of the peaks, the Fe_3O_4 components in the 26 F 5 h sample and the Fe_2O_3 ones in the 26 F 10 h sample were fitted using fixed parameters [24].

The 26 F 1 h spectrum (not reported) shows that all the iron is still present as Fe_2O_3 while, after 5 h milling, about half of the iron atoms forms new phases; magnetite and another component containing Fe(II) are detected. This last component gives an asymmetric broadened double peak, which can only be due to an amorphous material [25]. In fact, the two peaks have the same area but different amplitude and FWHM; the FWHM's are two times larger than that of a crystalline material. The isomer shift and quadrupole splitting of this component are in the range found in iron(II) containing silicate glasses with composition Fe_xSiO_{2+x} [26]. The amorphous phase was not evidenced by XRD because it only contributes to the diffracted intensities with a diffuse background. On the other hand, the presence of some wuestite, evidenced at this stage by XRD, cannot be ruled out in the Mössbauer spectrum because the peaks of the wuestite overlap with that of the amorphous component [24].

The formation of α-Fe and fayalite is observed at 10 hours [27]; only about 4% of the iron is still present as hematite while the amount of Fe(II), forming the

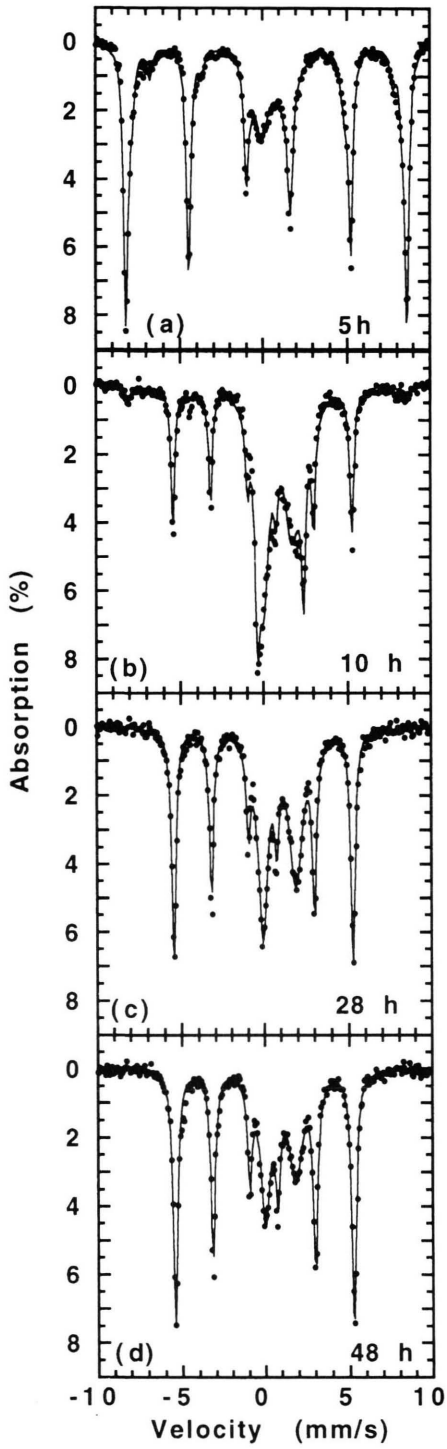

Fig. 3. Mössbauer absorption spectra at selected milling times for the 26 F sample. Experimental data are reported as dots; the solid line shows the fit.

Sample	Phase	δ mm/s	Δ mm/s	B T	$\Gamma_1/2$ mm/s	$\Gamma_2/2$ mm/s	Area %
26 F 5 h	Fe_2O_3	0.41	0.07	51.8	0.16		56
	Fe_3O_4 f.p.						20
	Fe_xSiO_{2+x} glass	0.76	1.37		0.85	0.49	24
26 F 10 h	Fe_2O_3 f.p.						4
	α-Fe	0.00		33.5	0.14		31
	Fe_xSiO_{2+x} glass	0.98	1.73		0.60	0.41	57
	Fe_2SiO_4	1.12	2.75		0.15		8
26 F 28 h	α-Fe	0.00		33.5	0.16		51
	Fe_xSiO_{2+x} glass	1.01	1.97		0.48	0.35	49
26 F 48 h	α-Fe	0.01		33.4	0.17		64
	Fe_xSiO_{2+x} glass	1.02	1.82		0.50	0.35	36

Table 1. Mössbauer parameters as obtained by fitting the spectra of the 26 F samples. Shown are the values of isomer shift (δ), quadrupole splitting (Δ), magnetic field (B), half width at half maximum of the peaks ($\Gamma_1/2$ and $\Gamma_2/2$) and absoprtion of each phase (Area). f.p. stands for fixed parameters.

amorphous phase, increases. After 28 hours, the sample contains about half of the iron atoms as α-Fe and the remaining as silicate glass; hematite and fayalite are no more detectable. At 48 hours, the sample is still composed of α-Fe and silicate glass but only one third of the iron is now present in the amorphous phase. The thermal treatment in H_2 flux has no detectable effect on the sample.

In all of the 26 F samples, the values of δ and Δ in the silicate glass are typical of Fe(II) in tetrahedral co-ordination [28, 29].

In the spectrum of the 26 F 48 h sample, shown in Fig. 4 a, the contribution of α-Fe was subtracted from the experimental data, in order to obtain the contribution of the silicate glass. The absorption of the glass, shown in Fig. 4 b, was fitted using one set of 25 Lorentzian doublets following the method of Viwel and Mørup. The Lorentzian FWHM was fixed to 0.22 mm/s; some trial fits led to the use of the values $\gamma = 1$ and β's $= 10$ for multipliers. Figure 4 c shows the probability distribution of the quadrupole splitting in the glass; the values of the free parameters of the fit are $\eta = +0.207$ and $\xi = 0.51$ mm/s.

Figure 5 shows the spectrum of the 41 F sample, as milled and after the thermal treatment in H_2 flux, while Table 2 reports the parameters obtained by a least squares fit with Lorentzian lines. In both samples α-Fe and Fe(II) silicates, in crystalline and amorphous state, are evidenced. The thermal treatment produces and increase of the fractions of α-Fe and the crystalline silicate Fe_2SiO_4, because a partial crystallization also occurs. The values of δ and Δ parameters for the silicate glass component are similar to those found in the 26 F samples, indicating that Fe(II) is in tetrahedral co-ordination.

The spectra of the 68 F sample, before and after the thermal treatment in H_2, are shown in Figure 6. The α-Fe phase is only evident in the spectrum of the reduced sample. The spectrum of the as milled sample presents a strong background which can be explained

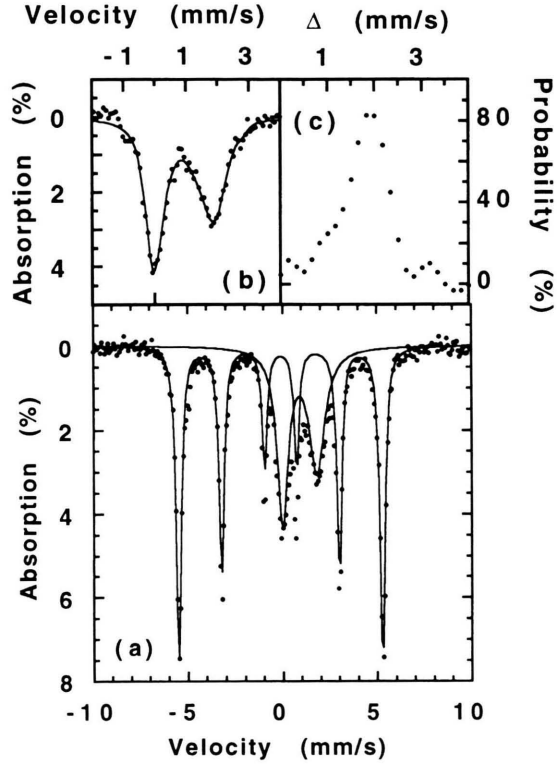

Fig. 4. Sample 26 F 48 h. (a) Mössbauer absorption spectrum. The solid line shows the component subspectra. (b) Absorption contribution due to the silicate glass. (c) Probability distribution of the quadrupole splitting in the glass.

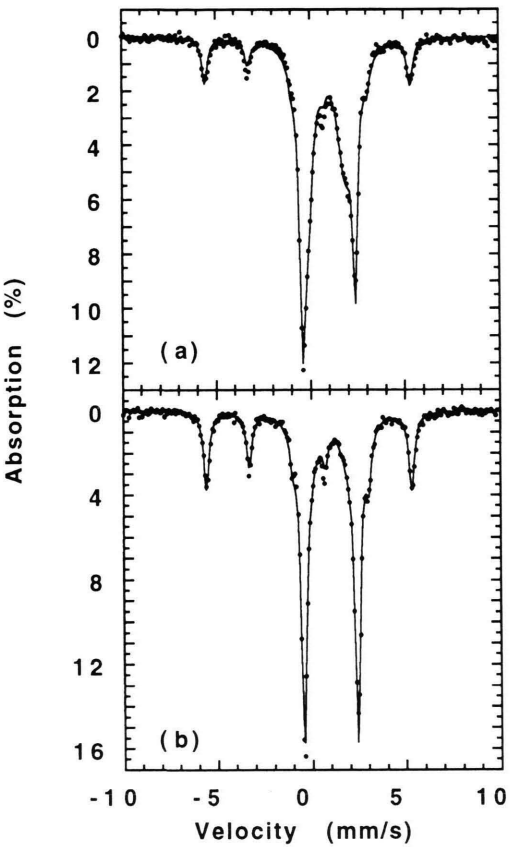

Fig. 5. Mössbauer absorption spectra for the 41 F sample at the end of the milling process (a) and after reduction in H_2 flux (b). Experimental data are reported as dots; the solid line shows the fit.

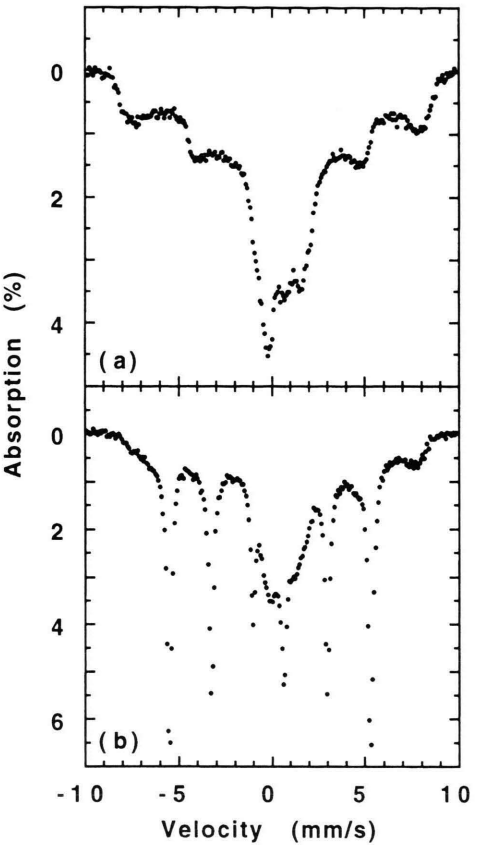

Fig. 6. Mössbauer absorption spectra for the 68 F sample at the end of the milling process (a) and after reduction in H_2 flux (b). Experimental data are reported as dots.

Sample	Phase	δ mm/s	Δ mm/s	B T	$\Gamma_1/2$ mm/s	$\Gamma_2/2$ mm/s	Area %
41 F	α-Fe	0.02		33.5	0.18		15
	Fe_xSiO_{2+x} glass	0.98	1.99		0.52	0.37	57
	Fe_2SiO_4	1.11	2.77		0.16		28
41 F reduced	α-Fe	0.01		33.5	0.18		29
	Fe_xSiO_{2+x} glass	1.06	1.99		0.50	0.47	18
	Fe_2SiO_4	1.12	2.81		0.18		53

Table 2. Mössbauer parameters as obtained by fitting the spectra of the 41 F samples. Shown are the values of isomer shift (δ), quadrupole splitting (Δ), magnetic field (B), half width at half maximum of the peaks ($\Gamma_1/2$ and $\Gamma_2/2$) and absoprtion of each phase (Area).

by the magnetic transition that occurs in hematite and magnetite at small particle size [30, 31]; both Fe_2O_3 and Fe_3O_4 give this kind of spectrum during the transition from the magnetically ordered state to the superparamagnetic one, when the average size of the particles is between 5 nm and 10 nm. The spectrum of the reduced sample still shows the magnetite together with α-Fe.

3. Discussion

On the basis of the intermediate compounds observed in the evolution of the reaction between Fe_2O_3 and Si, the following steps for the oxygen transfer reaction path from iron to silicon can be suggested:

1) $2\,Fe_2O_3 + Si \leftrightarrow 4\,FeO + SiO_2$,
$FeO + Fe_2O_3 \leftrightarrow Fe_3O_4$.

2) $2\,FeO + SiO_2 \leftrightarrow Fe_2SiO_4$,
$xFeO + SiO_2 \leftrightarrow Fe_xSiO_{2+x}$,
$FeO + Si \leftrightarrow Fe + SiO_2$.

3) $Fe_3O_4 + 2\,Si \leftrightarrow 3\,Fe + 2\,SiO_2$,
$Fe_2SiO_4 + Si \leftrightarrow 2\,Fe + 2\,SiO_2$,
$Fe_xSiO_{2+x} + x/2\,Si \leftrightarrow xFe + x/2\,SiO_2$.

The conversion of Fe_2O_3 into FeO (reduction from Fe(III) to Fe(II)) is certainly an essential step for the formation of the Fe(II) intermediate compounds which have been identified during the milling process. In fact, magnetite and Fe(II) silicate phases can only form through a reaction of FeO with either a reagent (Fe_2O_3) or a product of the oxygen displacement reaction (SiO_2) (step 2). Once FeO is formed, it easily reacts, so that it is hardly isolated; in fact, faint traces of this phase are only detected at 10 h milling. Among the variety of Fe(II) compounds obtained in the milling process, crystalline $FeSiO_3$ has never been observed, in disagreement with other authors who claim to have obtained this phase [15].

If the Si content is large enough, the Fe(II) compounds can be reduced to Fe(0) either through their decomposition followed by a reduction of FeO or through a direct reduction with residual Si (step 3).

The final products of solid state reaction depend on the proportion of Fe_2O_3 in the starting mixture. In the 26 F sample, which contains a stoichiometric amount of Si, step 3 reactions are dominant. Nevertheless, when a steady state is reached at the end of the milling process, about one third of the iron is still present as Fe(II) in the amorphous silicate. This quantity corresponds to an amount of unreacted Si equal to about 5% of the mixture weight, which may be undetected by XRD [32]. No further reduction is achieved after the following thermal treatment in H_2 flux. The final product is therefore a nanocomposite constituted by α-Fe nanocrystals in an amorphous matrix.

Complete reduction of Fe_2O_3 to Fe(0) by solid state reaction with a stoichiometric quantity of Al has been reported [16]. The different behaviour observed in the reaction with Si might be due to the smaller ΔG of this reaction (-64 kcal/at$_{Fe}$ for the reduction with Si and -100 kcal/at$_{Fe}$ for the reduction with Al).

In the 68 F sample, where Fe_2O_3 is present in large excess with respect to Si, Fe(0) cannot be obtained and only a partial reduction of Fe(III) to Fe(II) is possible at the end of the milling process. The formation of the Fe_3O_4 phase, containing both Fe(III) and Fe(II), is only observed in this case. In the as milled 41 F sample, a certain amount of Fe(0) is obtained together with a significant quantity of crystalline Fe_2SiO_4 and iron silicate glass. The following thermal treatment in H_2 flux only gives rise to an incomplete reduction of Fe(II) intermediate compounds.

4. Conclusion

The reduction of hematite with silicon induced by ball milling takes place through the formation of intermediate phases containing divalent iron; the phases are oxides (magnetite and wuestite) and silicates (fayalite and an iron silicate glass). In the stoichiometric sample (26 F), the reduction is not complete; the final product contains the iron as α-Fe nanocrystals and divalent iron in a silicate glass. In the samples with an excess of Fe_2O_3, the final products of ball milling and reduction processes also contains fayalite and magnetite.

Acknowledgements

The authors would like to thank Mr. Ivan Atzeni for technical assistance. The financial support of CNR and MURST is gratefully acknowledged.

[1] C. L. Chien, NATO ASI Ser. B **259,** 477 (1991).
[2] C. L. Chien, J. Appl. Phys. **69,** 5267 (1991).
[3] S. Komarneni, J. Mater. Chem. **2,** 1219 (1992).
[4] R. Roy, Mat. Res. Soc. Symp. Proc. **286,** 241 (1993).
[5] D. Chakravorty, Bull. Mater. Sci. **15,** 411 (1991).
[6] R. E. Newnham and S. E. Trolier-McKinstry, Ceram. Trans. **8,** 235 (1990).
[7] S. Roy, D. Das, D. Chakravorty, and D. C. Agarwal, J. Appl. Phys. **74,** 4746 (1993).
[8] S. Roy and D. Chakravorty, J. Mater. Res. **9,** 2314 (1993).
[9] J. P. Wang and H. L. Luo, J. Appl. Phys. **75,** 7425 (1994).
[10] R. D. Shull, J. J. Ritter, A. J. Shapiro, L. J. Swartzendruber, and L. J. Bennett, Mat. Res. Soc. Symp. Proc. **132,** 179 (1989).
[11] T. Ambrose, A. Gavrin, and C. L. Chien, J. Magn. Magn. Mater. **116,** L311 (1992).
[12] S. Linderoth and M. S. Pedersen, Appl. Phys. **75,** 5867 (1994).
[13] C. de Julian, A. K. Giri, M. P. Morales, and J. M. Gonzáles, Scripta Metall. Mater. **33,** 1079 (1995).

[14] G. B. Schaffer and P. G. McCormick, Metall. Trans. **A 21,** 2789 (1990).
[15] P. Matteazzi and G. L. Le Caër, Hyperf. Inter. **68,** 177 (1991).
[16] D. Bassett, P. Matteazzi, and F. Miani, Mater. Sci. Eng. **A 168,** 149 (1993).
[17] M. Pardavi-Horvath and L. Takacs, J. Appl. Phys. **73,** 6958 (1993).
[18] L. Takacs, Nanostr. Mater **2,** 241 (1993).
[19] L. Takacs and M. Pardavi-Horvath, J. Appl. Phys. **75,** 5864 (1994).
[20] B. E. Warren, X-Ray Diffraction, Addison-Wesley, Reading, Massachusetts 1969, p. 264.
[21] J. Hesse and A. Rubartsch, J. Phys. E, **7,** 526 (1974).
[22] C. Wivel and S. Mørup, J. Phys. E, **14,** 605 (1981).
[23] PDF file, International Center for Diffraction Data, 1601 Park Lane, Swarthmore, PA.
[24] J. Danon, in Chemical Applications of Mössbauer Spectroscopy, eds. V. I. Goldanskii and R. H. Herber, Academic Press, New York 1968, p. 159.
[25] G. Concas, F. Congiu, C. Muntoni, and G. Pinna, J. Phys. Chem. Solids **56,** 877 (1995).
[26] M. Guglielmi, A. Maddalena, and G. Principi, J. Mater. Science Lett. **2,** 467 (1983).
[27] J. Ito and S. S. Hafner, Amer. Mineral. **59,** 700 (1974).
[28] M. Darby Dyar, Amer. Mineral. **70,** 304 (1985).
[29] J. M. D. Coey, J. Physique **35,** C6-89 (1974).
[30] A. M. van der Kraan, Phys. Stat. Solidi (a) **18,** 215 (1985).
[31] S. Mørup, H. Topsøe, and J. Lipka, J. Physique **37,** C6-287 (1976).
[32] H. P. Klug and L. E. Alexander, X-Ray Diffraction Procedures, Wiley, New York 1974, p. 524.